

RESEARCH ARTICLE

Centrosome maturation requires phosphorylation-mediated sequential domain interactions of SPD-5

Momoe Nakajo, Hikaru Kano, Kenji Tsuyama, Nami Haruta* and Asako Sugimoto*

ABSTRACT

Centrosomes consist of two centrioles and the surrounding pericentriolar material (PCM). The PCM expands during mitosis in a process called centrosome maturation, in which PCM scaffold proteins play pivotal roles to recruit other centrosomal proteins. In *Caenorhabditis elegans*, the scaffold protein SPD-5 forms a PCM scaffold in a polo-like kinase 1 (PLK-1) phosphorylation-dependent manner. However, how phosphorylation of SPD-5 promotes PCM scaffold assembly is unclear. Here, we identified three functional domains of SPD-5 through *in vivo* domain analyses, and propose that sequential domain interactions of SPD-5 are required for mitotic PCM scaffold assembly. Firstly, SPD-5 is targeted to centrioles through a direct interaction between its centriole localization (CL) domain and the centriolar protein PCMD-1. Then, intramolecular and intermolecular interactions between the SPD-5 phospho-regulated multimerization (PReM) domain and the PReM association (PA) domain are enhanced by phosphorylation by PLK-1, which leads to PCM scaffold expansion. Our findings suggest that the sequential domain interactions of scaffold proteins mediated by PLK-1 phosphorylation is an evolutionarily conserved mechanism of PCM scaffold assembly.

This article has an associated First Person interview with the first author of the paper.

KEY WORDS: Centrosome maturation, PCM scaffold assembly, *C. elegans*, SPD-5, Polo-like kinase, PCMD-1

INTRODUCTION

Centrosomes, the major microtubule organizing centers (MTOCs) in animal cells, consist of two centrioles and a surrounding amorphous mass of proteins called the pericentriolar material (PCM). The size of the PCM dramatically changes in a cell-cycle dependent manner. During interphase, a small amount of PCM is assembled adjacent to the centrioles. When cells enter mitosis, centrosomal proteins including γ -tubulin complexes are recruited to the PCM to expand its size and increase its microtubule nucleation activity. This process is called centrosome maturation (Palazzo et al., 2000).

During centrosome maturation, PCM scaffold proteins play pivotal roles to recruit other centrosomal proteins around centrioles. One of the well-characterized PCM scaffold proteins is Centrosomin (Cnn) in *Drosophila melanogaster* and its ortholog CDK5RAP2 in

humans (Megraw et al., 1999; Fong et al., 2008). In *Caenorhabditis elegans*, SPD-5 is thought to be a functional homolog of Cnn/CDK5RAP2, even though sequence homology is undetectable (Hamill et al., 2002). These functional homologs contain multiple predicted coiled-coil regions, and scaffold assembly of these proteins is facilitated by the interaction with the conserved coiled-coil proteins SPD-2 (also known as Cep192 in humans) and phosphorylation by the polo-like kinase 1 (PLK-1; also known as PLK1 in humans, Polo in *Drosophila*) (Conduit et al., 2014a; Decker et al., 2011; Giansanti et al., 2008; Gomez-Ferrera et al., 2007; Haren et al., 2009; Kemp et al., 2004; Pelletier et al., 2004). These similarities suggest that a universal mechanism of PCM scaffold assembly might exist.


Through studies of Cnn, its distinct domains and their roles in scaffold assembly have been identified. Cnn has two motifs that are conserved in CDK5RAP2; the N-terminal Centrosomin motif 1 (CM1) domain that recruits γ -tubulin complexes to the centrosomes (Fong et al., 2008; Zhang and Megraw, 2007), and the C-terminal CM2 domain that is implicated in centrosomal targeting (Barr et al., 2010; Feng et al., 2017). During early mitosis in *Drosophila*, Cnn is recruited to the centrioles mainly by Spd-2, then phosphorylated by Polo at the central region called the phospho-regulated multimerization (PReM) domain (Alvarez-Rodrigo et al., 2019; Conduit et al., 2014a, b). The phosphorylation of the PReM domain enhances the interaction between this domain and the CM2 domain. This phosphorylation-dependent conformational change of Cnn leads to the assembly of the PCM scaffold (Feng et al., 2017).

In *C. elegans*, PCM scaffold protein SPD-5 is recruited to centrioles by centriolar/PCM protein SPD-2, and they depend on each other for localization to the expanded PCM (Hamill et al., 2002; Kemp et al., 2004; Pelletier et al., 2004). SPD-2 also functions as a PLK-1 recruiter, and PLK-1 phosphorylation activity is required for centrosome maturation (Decker et al., 2011; Erpf et al., 2019). The mutation of the PLK-1 phosphorylation sites in the SPD-5 central region results in the failure of scaffold assembly *in vivo* and *in vitro* (Woodruff et al., 2015; Wueseke et al., 2016). *In vitro* reconstitution studies have further demonstrated that purified SPD-5 assembles into spherical condensates which can recruit other downstream PCM proteins. This SPD-5 scaffold assembly is robustly promoted by the addition of SPD-2 and PLK-1 (Woodruff et al., 2017, 2015). Recently, the centriolar/PCM protein PCMD-1 was identified as a novel factor involved in PCM organization. Genetic analyses have indicated that PCMD-1 is required for the recruitment of SPD-5 around centrioles and the integrity of the PCM scaffold (Erpf et al., 2019). Although the involvement of SPD-2, PCMD-1 and PLK-1 is implicated, how SPD-5 interacts with each of these proteins and is regulated by phosphorylation in the PCM scaffold assembly is poorly understood.

In this study, we conducted *in vivo* domain analysis of SPD-5 and identified three functional domains. We propose a model for SPD-5 scaffold assembly during centrosome maturation through sequential

Laboratory of Developmental Dynamics, Graduate School of Life Sciences, Tohoku University, 2-1-1 Katahira, Aoba-ku, Sendai 980-8577, Japan.

*Authors for correspondence (asugimoto@tohoku.ac.jp; nami.haruta.c5@tohoku.ac.jp)

 M.N., 0000-0003-3158-542X; H.K., 0000-0001-7033-1129; K.T., 0000-0003-4698-9961; N.H., 0000-0002-4232-9635; A.S., 0000-0001-6001-4293

Handling editor: Guangshuo Ou
Received 16 June 2021; Accepted 18 March 2022

interactions of these domains mediated by PLK-1-dependent phosphorylation.

RESULTS

Regions in the C-terminal half of SPD-5 are involved in PCM localization

To understand the mechanism(s) by which SPD-5 is localized to the centrosomes and participates in PCM scaffold formation, we conducted a domain analysis of SPD-5 *in vivo* (Fig. 1A). Several truncated versions of SPD-5 proteins tagged with green fluorescent protein (GFP) at their N-terminus were expressed in early *C. elegans* embryos from a transgene inserted into the specific locus on Chromosome II that is distinct from the *spd-5* locus. The localization of transgenic proteins and embryonic phenotypes were investigated in the presence and the absence of endogenous SPD-5. The expression of each SPD-5 fragment was confirmed by measuring the GFP signal intensity of whole embryos and western blotting of worm extracts (Fig. 1B; Fig. S1A).

In both the presence and absence of endogenous SPD-5, the full-length SPD-5 [GFP::SPD-5(FL); amino acids (aa) 1–1198] localized to the centrosomes throughout the cell cycle in all observed early embryos, as previously reported (Woodruff et al., 2015) ($n=15$ and 21 , respectively) (Fig. 1A). As GFP::SPD-5(FL) fully rescued the embryonic lethality of *spd-5(RNAi)* ($n=21$), we concluded that this fusion protein is functional *in vivo*. However, we noted that in the absence of the endogenous SPD-5, the shape of the centrosomal signal was slightly distorted, which might be caused by the lower amount of GFP::SPD-5(FL) relative to that of endogenous SPD-5 (Fig. S1A) and/or the effect of the GFP tag.

We first divided the SPD-5 protein into two regions, the N-terminal half (N-half, aa 1–522) and the C-terminal half (C-half, aa 523–1198) (Fig. 1A). In all observed embryos, the GFP::SPD-5(N-half) signal was barely detected at centrosomes in either the presence ($n=10$) or absence ($n=5$) of endogenous SPD-5, although in the latter case some condensates were detected in the cytosol at prometaphase to anaphase (Fig. S1B).

In contrast, GFP::SPD-5(C-half) localized to the centrosome in the presence of endogenous SPD-5 (100%, $n=11$) (Fig. 1A). In the absence of endogenous SPD-5, the centrosomal signal of GFP::SPD-5(C-half) became weaker and smaller, indicative of its centriolar localization (100%, $n=15$) (Fig. 1A,C). Our observation that GFP::SPD-5(C-half) is insufficient for the full expansion of the PCM implies the involvement of the N-half region in PCM scaffold assembly. However, GFP::SPD-5(C-half) can interact with endogenous SPD-5 to localize to the centrosomes, suggesting that the C-terminal half of SPD-5 is involved in its targeting to the centrioles and interacts with endogenous SPD-5.

SPD-5(C1) has a dominant-negative effect on PCM scaffold formation by endogenous SPD-5

We further dissected the SPD-5 C-terminal half for its ability to interact with SPD-5 itself and its function in centriolar targeting. When the last 272 residues of the C-terminal (C1) region, aa 927–1198) were deleted [GFP::SPD-5(Δ C1)], localization to the PCM and the centrioles was abolished in either the presence (100%, $n=4$) or absence (100%, $n=5$) of endogenous SPD-5 (Fig. 1A), suggesting that the C1 region is necessary for both self-interaction and centriolar localization.

In turn, the C1 region [GFP::SPD-5(C1)] localized to the centrosome in the presence of endogenous SPD-5 (100%, $n=9$; Fig. 1A), but the signal area was significantly smaller [27% of that of GFP::SPD-5(FL)] and was fragmented (Fig. 1D; Fig. S1C).

GFP::SPD-5(C1) accumulated around the centrioles in the presence of endogenous SPD-5 (Fig. 1A; Fig. S1C). Immunostaining using an antibody against SPD-5 (anti-SPD-5) that recognizes both endogenous SPD-5 and GFP::SPD-5(C1) revealed that endogenous SPD-5 colocalized with the disordered and fragmented signal of GFP::SPD-5(C1) (100%, $n=8$; Fig. 2A). Notably, this strain showed ~46% embryonic lethality (Fig. 2B). These results suggest that the C1 fragment disrupts the ability of endogenous SPD-5 to assemble the PCM scaffold in a dominant-negative manner.

In the absence of endogenous SPD-5, the GFP::SPD-5(C1) signal became even weaker and smaller (100%, $n=11$; Fig. 1A,C), implying that this region of SPD-5 localized only around the centrioles. These results suggest that the C1 region is involved in centriolar targeting and in intermolecular interactions with other SPD-5 molecules.

The C-terminal region of SPD-5 contains two functional domains

The C-terminal half of the C1 region contains a region that is highly conserved among the *Caenorhabditis* genus, which we refer to as the C2 region (aa 1061–1198). In the presence of endogenous SPD-5, GFP::SPD-5(C2) localized to the centrosome (100%, $n=8$), although the signal area was ~15% smaller than that of SPD-5(FL) (Fig. 1A,D). A further deletion of 30 residues (C3, aa 1091–1198) abolished this centrosomal localization (100%, $n=5$; Fig. 1A). Unlike GFP::SPD-5(C1), GFP::SPD-5(C2) did not show a dominant-negative effect, and the localization of endogenous SPD-5 was unaffected (Fig. 2A,B). This centrosomal localization of GFP::SPD-5(C2) was lost in the absence of SPD-5 (92%, $n=12$; Fig. 1A). Thus, the C2 region interacts with endogenous SPD-5 in the central region of the PCM, but it lacks the ability to independently localize around the centrioles.

The fragment lacking the majority of the C2 region [GFP::SPD-5(Δ C3)] localized around the centrioles in the presence of endogenous SPD-5 but failed to expand to the PCM (100%, $n=4$; Fig. 1A). This suggests that the C2 region is dispensable for centriolar localization but is necessary for incorporation into the PCM.

The remaining N-terminal half of the C1 region is referred to as the C4 region (aa 927–1060). In both the presence and absence of endogenous SPD-5, GFP::SPD-5(C4) localization was represented by very small signals, plausibly around the centrioles (92%, $n=13$; 100%, $n=12$, respectively) (Fig. 1A,C; Fig. S1C,D), suggesting that the C4 region by itself can localize to the centrioles, independently of the interaction with endogenous SPD-5. GFP::SPD-5(C4) did not show a dominant-negative effect on PCM scaffold assembly of endogenous SPD-5 (Fig. 2A,B).

Taken together, these results identified two functional regions in the C-terminal half of SPD-5: C2 (aa 1061–1198), which is involved in the intermolecular interaction with endogenous SPD-5, and C4 (aa 927–1198), which is necessary and sufficient for centriolar targeting.

The C4 region of SPD-5 physically interacts with the centriolar protein PCMD-1

To identify proteins involved in the recruitment of the SPD-5(C4) domain to the centrioles, we conducted a yeast two-hybrid screen. Using SPD-5(C1) as the bait, the centriolar protein PCMD-1 was identified. The interaction between SPD-5 and PCMD-1 has been reported previously (Stenzel et al., 2021). PCMD-1 also interacted with SPD-5(C4), but not with SPD-5(C2) (Fig. 3A). SPD-5(C4) interacted with the N-terminal half region of PCMD-1 (aa 1–242), which contains predicted coiled-coil and disordered regions (Fig. 3B).

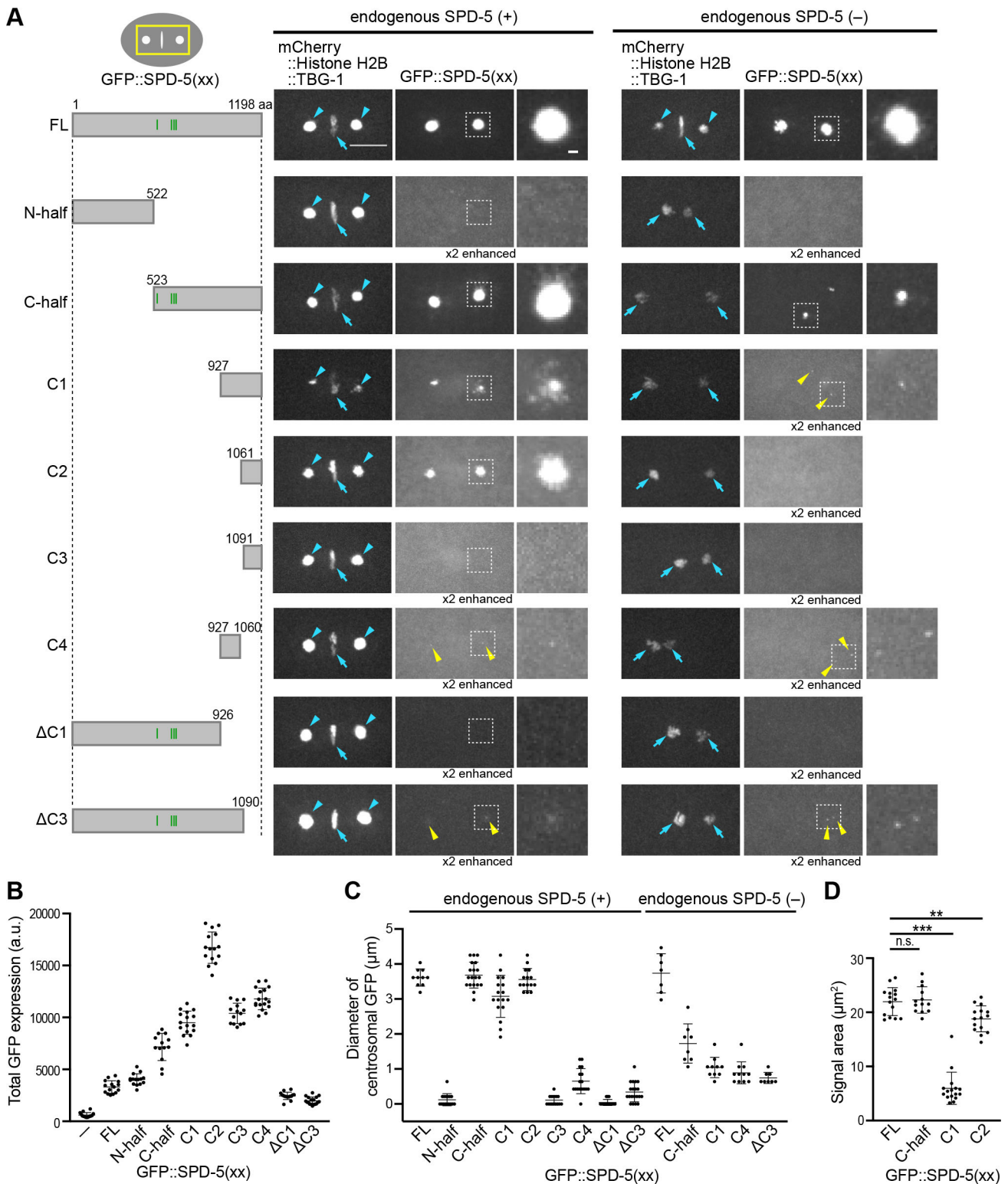


Fig. 1. See next page for legend.

Colocalization of PCMD-1 and the SPD-5(C4) domain was confirmed by immunostaining using the anti-PCMD-1 and anti-GFP antibodies. In the absence of endogenous SPD-5, both GFP::SPD-5(C4) and GFP::SPD-5(C1) colocalized with PCMD-1 on the centriole (100%, $n=18$; 100%, $n=18$, respectively), whereas GFP::SPD-5(C2) did not (100%, $n=16$; Fig. 3C). To verify that the

centriolar localization of SPD-5(C4) is dependent on PCMD-1, the localization of GFP::SPD-5(C4) was observed in the *pcmd-1(RNAi)* embryo. The centriolar localization of GFP::SPD-5(C4) significantly decreased in *pcmd-1(RNAi)* embryos (Fig. 3D,E) (peak values; $P<0.0001$, Welch's *t*-test). From these results, we concluded that the C4 region of SPD-5 is recruited to the centrioles

Fig. 1. *In vivo* domain analysis of SPD-5. (A) Images of *C. elegans* one-cell embryos that express full-length or truncated GFP::SPD-5 proteins [GFP::SPD-5(xx)], mCherry::Histone H2B and mCherry::TBG-1/ γ -tubulin. The gray boxes in the left column indicate the fragments used in the assay. The four green vertical lines indicate the serine residues that can be phosphorylated by PLK-1 (S530, S627, S653 and S658) (Woodruff et al., 2015). The areas around the centrosomes and chromosomes, illustrated as a yellow rectangle in the upper-left diagram, are shown in each image. The images were taken 160 s after nuclear envelope breakdown, which corresponds to metaphase in the control embryos. Scale bar: 10 μ m. Blue arrows indicate mCherry::Histone H2B (a chromosome marker), and blue arrowheads indicate mCherry::TBG-1 (a centrosome marker). Yellow arrowheads indicate the faint and small GFP signals on and around the centrioles. The magnified and enhanced images of the areas in the dotted white squares are shown in the right column. Scale bar: 1 μ m. Numbers of embryos with similar results as the shown images (from top to bottom): for the SPD-5(+) condition, 15/15, 10/10, 11/11, 9/9, 8/8, 5/5, 12/13, 4/4, 4/4; for the SPD-5(-) condition, 21/21, 5/5, 15/15, 11/11, 11/12, 11/11, 12/12, 5/5, 6/6. (B) Expression levels of GFP-labeled truncated versions of SPD-5 indicated by the total GFP signal intensity (displayed in arbitrary units, a.u.) in whole one-cell metaphase embryos expressing each GFP::SPD-5(xx). In the first lane, '-' indicates wild-type worms. Bars indicate the mean \pm s.d. $n=15, 15, 15, 13, 16, 15, 14, 17, 15, 18$ (from left to right). (C) Diameter of centrosomal GFP signals for each GFP::SPD-5(xx) in the presence or the absence of endogenous SPD-5 at 160 s after nuclear envelope breakdown, which corresponds to metaphase in the control embryos. The mean \pm s.d. is indicated. $n=15, 15, 13, 16, 15, 14, 17, 15, 18, 7, 8, 10, 11, 8$ (from left to right). (D) Area of centrosomal GFP signals for each GFP::SPD-5(xx) in the presence of endogenous SPD-5 at metaphase. The mean \pm s.d. is indicated. ** $P<0.01$; *** $P<0.001$; n.s., not significant ($P\geq 0.05$), Tukey's multiple comparisons test. $n=15, 13, 16, 15$ (from left to right).

by PCMD-1 through direct interaction. The C4 region is hereafter called the CL (centriole localization) domain.

Additionally, a yeast two-hybrid screen using PCMD-1 as the bait identified the centrosomal proteins TAC-1, PLK-1 and PLK-2 (Fig. S2). The interaction between PCMD-1 and PLK-1 has recently been reported (Stenzel et al., 2021).

The C2 region of SPD-5 interacts with the phosphorylated SPD-5 central region

Next, we examined which region of SPD-5 interacts with the C2 region by yeast two-hybrid assays. The C2 region (and the C1 region, which contains C2) interacted with the middle region of SPD-5 (aa 272–732) (Fig. 4A). The shorter fragments SPD-5(272–680), SPD-5(400–680) and SPD-5(523–732) did not interact with the C2 region (Fig. 4A), implying that a relatively long (~460 aa) central region is required for the interaction with the C2 region.

As SPD-5(272–732) contains the PLK-1 phosphorylation sites (S530, S627, S653 and S658) required for the expansion of the SPD-5 scaffold (Woodruff et al., 2015; Wueseke et al., 2016), we next examined by pull-down assays whether their phosphorylation by PLK-1 affects the interaction with SPD-5(C2). Purified glutathione *S*-transferase (GST)-tagged SPD-5(272–732) proteins with or without PLK-1 pre-treatment were incubated with purified SPD-5(C2) proteins (all proteins used are shown in Fig. S3A,B). The interaction of SPD-5(C2) with wild-type SPD-5(272–732_WT) or phosphoresistant SPD-5(272–732_4A) (containing the S530A, S627A, S653A and S658A mutations) significantly increased by PLK-1 phosphorylation (Fig. 4B), but interaction with SPD-5(272–732_4A) was ~25% lower than that with SPD-5(272–732_WT). These results imply that PLK-1-phosphorylation in SPD-5(272–732) at multiple residues, including the four serine residues, strongly enhances C2 binding.

To verify that the centrosomal localization of SPD-5(C2) is dependent on the interaction with phosphorylated SPD-5 by PLK-1,

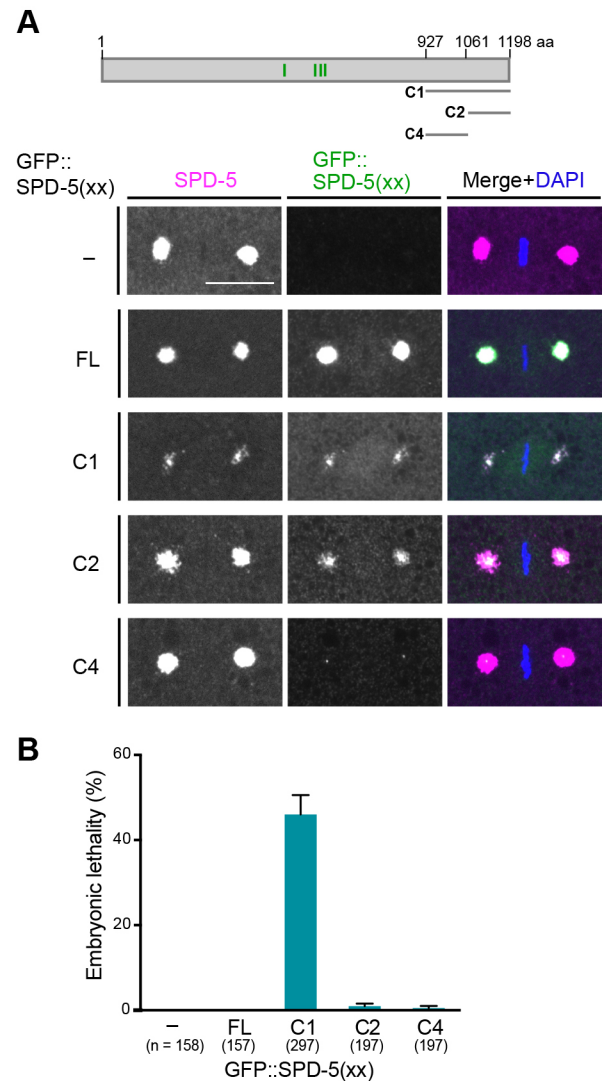


Fig. 2. GFP::SPD-5(C1) has a dominant-negative effect on PCM scaffold formation by endogenous SPD-5. (A) Immunostaining of wild-type embryos and embryos expressing GFP::SPD-5(xx) using anti-SPD-5 and anti-GFP antibody. The top diagram indicates the fragments used. The four green vertical lines indicate serine residues that can be phosphorylated by PLK-1. The anti-SPD-5 antibody stains both endogenous SPD-5 and each GFP::SPD-5(xx). Scale bar: 10 μ m. Numbers of embryos with similar results as the shown images (from top to bottom): 9/9, 12/12, 8/8, 8/8, 8/8. (B) Embryonic lethality of each GFP::SPD-5(xx)-expressing strain. Values indicate mean \pm s.e.m. n -values are indicated underneath the x -axis.

the localization of full-length or truncated SPD-5 fragments [GFP::SPD-5(xx)] was observed in the absence of PLK-1 activity. Embryos permeabilized by *perm-1(RNAi)* were treated with the PLK-1 inhibitor BI-2536 to inactivate PLK-1, or the solvent DMSO. SPD-5 fragments that contain the CL domain [GFP::SPD-5(FL), GFP::SPD-5(C1) and GFP::SPD-5(C4)] localized to the centrioles in the absence of PLK-1 activity (100%, $n=28$; 100%, $n=25$; 100%, $n=27$, respectively) (Fig. 4C,D). We noted that the amount of GFP::SPD-5(C1) localized to centrioles was higher than that of GFP::SPD-5(FL) or GFP::SPD-5(C4) (Fig. 4D). GFP::SPD-5(FL) localization around the centrioles also indicated that a small amount of endogenous SPD-5 remained around the centrioles even after PLK-1 inhibition. On the other hand, GFP::SPD-5(C2) that lacks the CL domain did not show any localization (77%, $n=31$), or showed

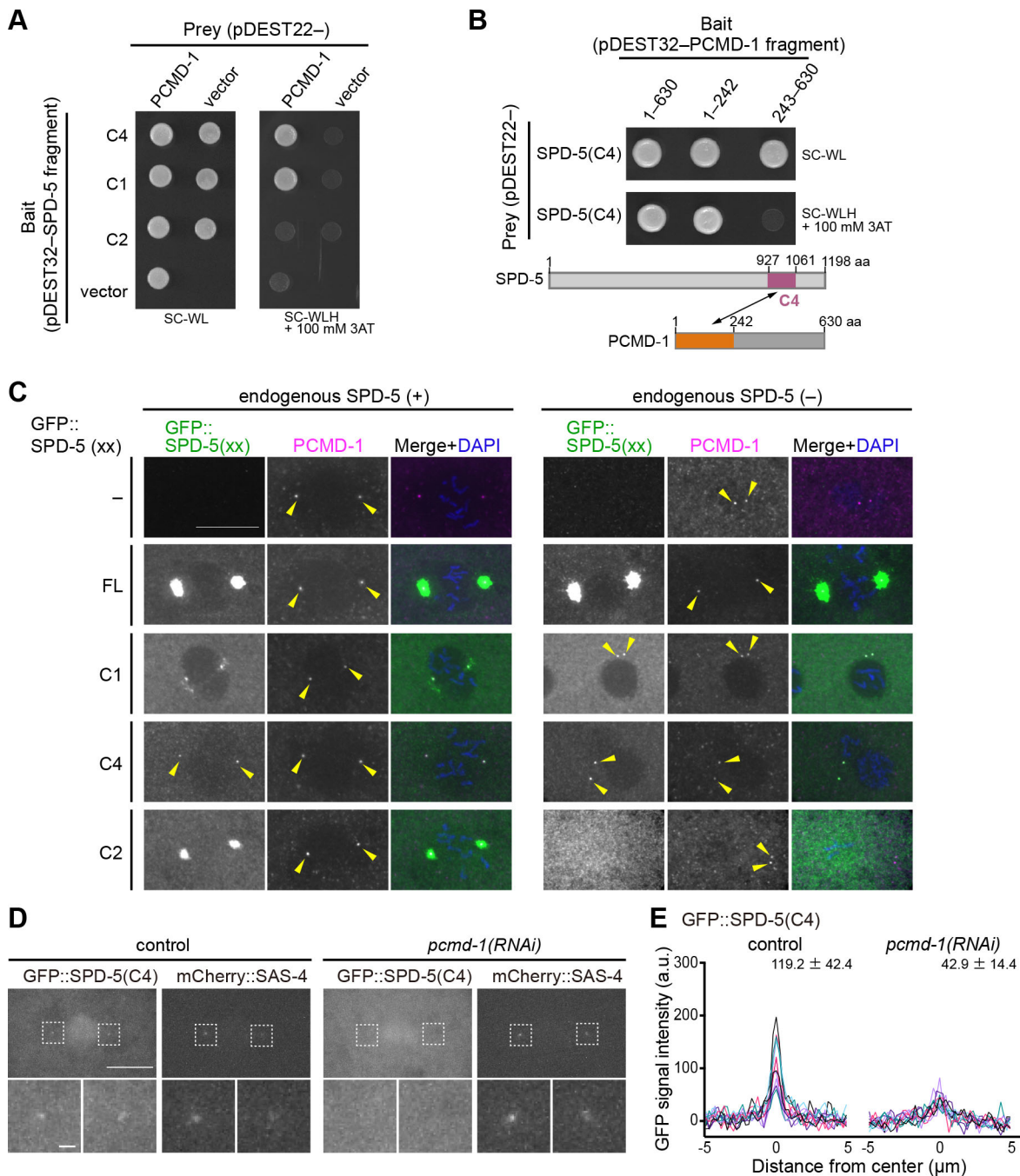


Fig. 3. SPD-5(C4) is recruited to centrosomes by PCMD-1 through direct interaction. (A,B) Yeast two-hybrid analyses of interactions between SPD-5 and PCMD-1. Growth on SC-Trp-Leu plates (SC-WL, control) and SC-Trp-Leu-His plates (SC-WLH) containing 100 mM 3-amino-1,2,4-triazol (3AT) is shown. Assessment of PCMD-1 interactions with SPD-5(C4), SPD-5(C1) and SPD-5(C2) is shown in A. Analysis of PCMD-1 interactions with SPD-5(C4) is shown in B. (C) Colocalization of SPD-5(xx) and PCMD-1 in one-cell embryos. Embryos were immunostained using anti-GFP and anti-PCMD-1 antibodies. Images of one-cell embryos at the stages from pronuclear migration to prometaphase are shown. Yellow arrowheads indicate the small PCMD-1 or GFP signals on and around the centrosomes. Scale bar indicates 10 μm. Numbers of centrosomes with similar results as the shown images (from top to bottom): for the SPD-5(+) condition, 14/14, 16/16, 16/16, 18/18, 18/18; for the SPD-5(-) condition, 14/14, 14/14, 18/18, 18/18, 16/16. (D) Localization of GFP::SPD-5(C4) in *pcmd-1(RNAi)* embryos. Images of the areas around the centrosomes and chromosomes in one-cell embryos that express GFP::SPD-5(C4) and mCherry::SAS-4 (a centriole marker) are shown (top). Images (bottom) are magnified views of the areas indicated by white squares. Scale bars: 10 μm (top), 1 μm (bottom). (E) Signal distribution of GFP::SPD-5(C4) at centrosomes in control or *pcmd-1(RNAi)* embryos. a.u., arbitrary units. The peak values (mean±s.d.) are indicated. $n=11$ for each condition.

weak centriolar localization (23%) (Fig. 4C,D). These results indicate that GFP::SPD-5(C2) localizes to the centrosomes through interaction with endogenous PLK-1-phosphorylated SPD-5.

These *in vivo* and *in vitro* domain analyses revealed two functional regions of SPD-5 (Fig. 5A). The SPD-5(272–732)

region, which contains the key PLK-1 phosphorylation sites and was essential for SPD-5 scaffold expansion, is the PReM domain, named after the Centrosomin PReM domain in *Drosophila* (Conduit et al., 2014a). The C2 region, which was necessary and sufficient for the phosphorylation-dependent interaction with

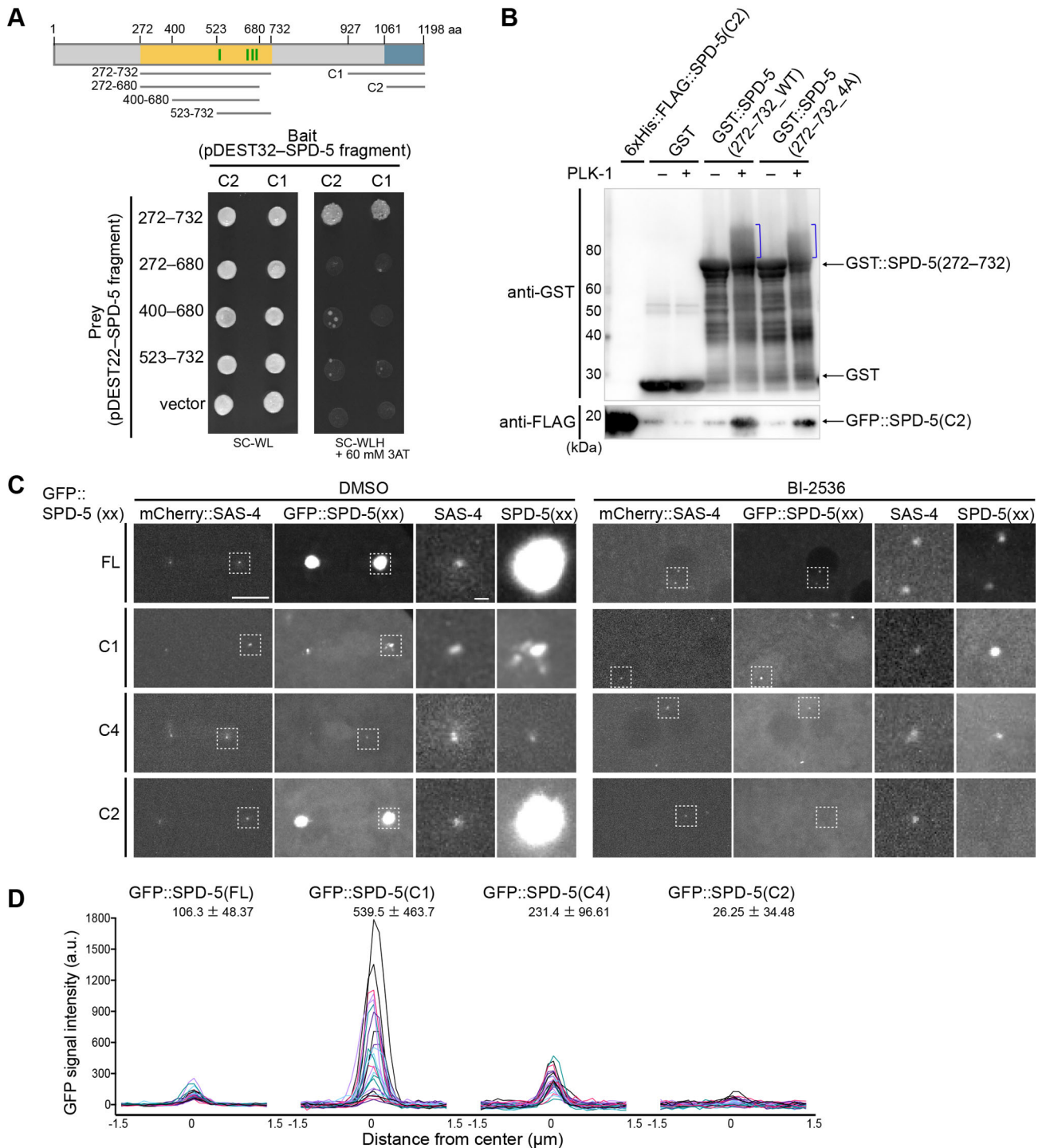


Fig. 4. SPD-5(C2) interacts with the central region of SPD-5 in a PLK-1 phosphorylation-dependent manner. (A) Yeast two-hybrid analysis of interactions between SPD-5 fragments. The upper diagram shows the region corresponding to each SPD-5 fragment. The four green vertical lines indicate serine residues that can be phosphorylated by PLK-1. The growth of each yeast strain on SC-Trp-Leu plates (SC-WL, control) and SC-Trp-Leu-His plates (SC-WLH) containing 60 mM 3-amino-1,2,4-triazol (3AT) is shown. (B) Pull-down assay for the phosphorylation-dependent interaction between SPD-5(C2) and SPD-5(272-732). Western blotting using the anti-GST and anti-FLAG antibodies is shown. Pre-incubation of each GST-tagged protein with PLK-1 is indicated by '+' or '-'. Blue brackets correspond to phosphorylated GST::SPD-5(272-732_WT) and GST::SPD-5(272-732_4A) by PLK-1 (Fig. S3B). Since SPD-5(272-732) has been shown to contain other phosphorylation sites than the mutated sites (Woodruff et al., 2015), SPD-5(272-732_4A) would still be phosphorylated by PLK-1. 6xHis::FLAG::SPD-5(C2), 19.2 kDa; GST::SPD-5(272-732_WT), 78.2 kDa; GST::SPD-5(272-732_4A), 78.1 kDa; GST, 26.8 kDa. $n=2$. (C) *In vivo* PLK-1 inhibition assay. Images of the areas around the centrosomes and chromosomes in one-cell embryos that express full-length or truncated GFP::SPD-5 proteins [GFP::SPD-5(xx)] and mCherry::SAS-4 (a centriole marker), after 15 min treatment with DMSO or the PLK-1 inhibitor, BI-2536, at pronuclear appearance are shown. Images in the right columns are magnified views of the areas indicated by white squares. Scale bars: 10 μm (left columns), 1 μm (right columns). Numbers of centrosomes that showed similar results (from top to bottom): for DMSO condition, 22/22, 22/22, 26/26, 26/26; for BI-2536 condition, 28/28, 25/25, 27/27, 31/31 [not localized to centrosomes (24/31), showed weak localization (7/31)]. (D) Signal distribution of GFP::SPD-5(xx) at centrosomes in BI-2536 treated embryos. a.u., arbitrary units. The peak values (mean±s.d.) are indicated. $n=28, 25, 27, 31$.

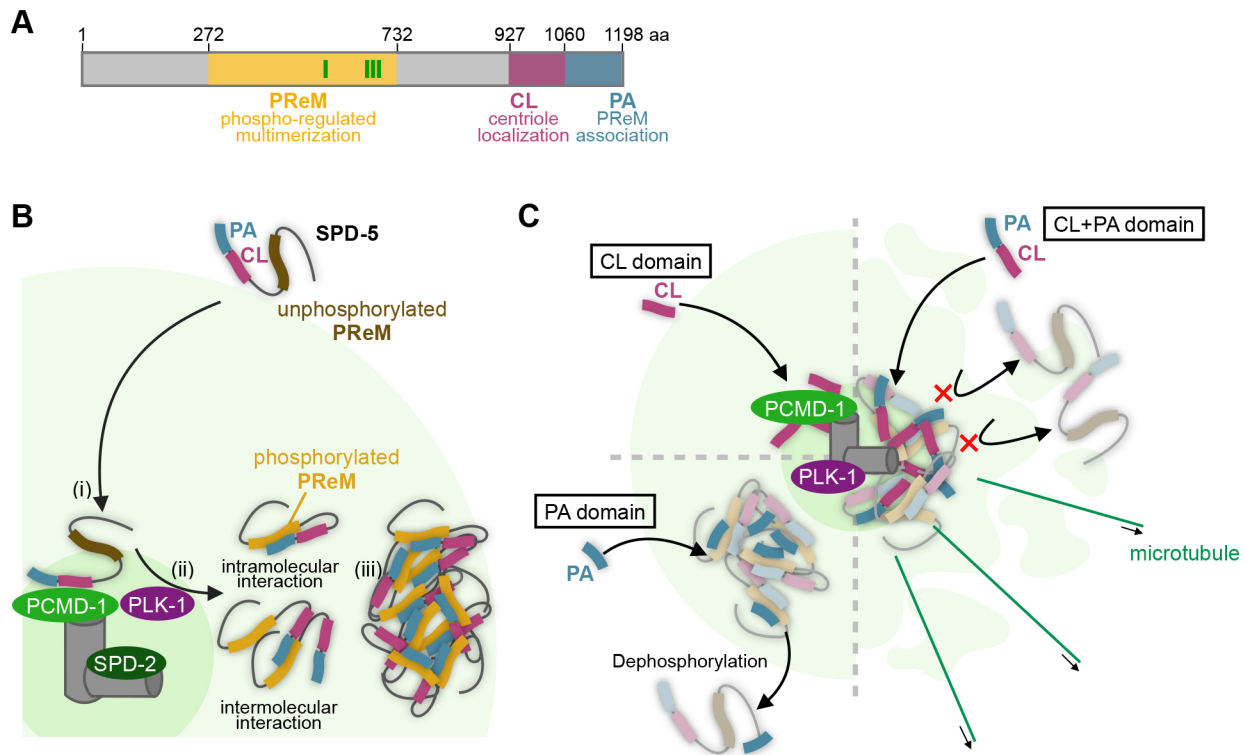


Fig. 5. A model for PCM scaffold assembly by SPD-5. (A) The three functional domains of SPD-5 identified in this study are indicated. (B) A model of PCM scaffold assembly by SPD-5 through PLK-1 phosphorylation-dependent interactions. See text for details about steps i–iii. (C) Interpretation of the phenotypes of the CL, PA and CL+PA fragments observed in our *in vivo* analysis. The CL fragment localizes to centrioles through the interaction with centriolar PCMD-1. The PA fragment interacts with the phosphorylated PReM domain of endogenous SPD-5 and localizes to the central region of PCM. The CL+PA fragment accumulates around the centrioles with endogenous SPD-5 and might prevent scaffold expansion or the connection between centrioles and PCM, which weakens the PCM that could be ripped apart by microtubule-mediated pulling forces.

SPD-5(272–732) (PReM) is referred to as the PReM association (PA) domain.

DISCUSSION

A model for how SPD-5 proteins assemble into the mitotic PCM scaffold

Here, we propose a model for SPD-5 scaffold formation during centrosome maturation (Fig. 5B). (i) SPD-5 is recruited to the centrosomes through the interaction between its CL domain and PCMD-1, which is localized to the centrioles (Erpf et al., 2019). (ii) As PCMD-1 interacts with both SPD-5 and PLK-1 (this study and Stenzel et al., 2021), this interaction promotes phosphorylation of the PReM domain of SPD-5 by PLK-1 in the vicinity of the centrioles. The phosphorylated PReM domain interacts with the PA domain of the same and/or other SPD-5 molecules. (iii) This interaction between the phosphorylated PReM domain and the PA domain promotes SPD-5 multimerization to expand the PCM scaffold.

We speculate that both intermolecular and intramolecular interactions between the PA domain and the phosphorylated PReM domain are involved in PCM formation. The intermolecular interaction is indicated by the localization of GFP::SPD-5(PA) to the PCM in the presence of endogenous SPD-5. The requirement of intramolecular interaction is indicated by the result that GFP::SPD-5(Δ C3) that contains the PReM domain but not the PA domain did not expand to the PCM even though it localized to the centrioles. A previous study (Wueske et al., 2016) showed that the phosphoresistant mutant of SPD-5 [SPD-5(4A)] could not form the mitotic PCM by itself even though it could localize to the PCM in

the presence of endogenous SPD-5, which is consistent with our model that the intramolecular and intermolecular interaction between the PA domain and the phosphorylated PReM domain is crucial for PCM expansion.

We noted some discrepancies between the *in vitro* and *in vivo* data. Our *in vitro* assay showed the interaction between PLK-1-treated SPD-5(272–732_{WT} and 4A) (PReM) and SPD-5(C2) (PA) fragments (Fig. 4B). However, GFP::SPD-5(Δ C1) and GFP::SPD-5(Δ C3) that contain the PReM domain did not localize to the PCM in the presence of endogenous SPD-5 in early embryos (Fig. 1A). These discrepancies might be explained by the difference in protein concentrations between the *in vitro* and *in vivo* experiments. In our *in vitro* assay, high concentrations of purified SPD-5 fragments were incubated in the absence of other proteins, which might be preferable for the protein interactions than physiological conditions. In the *in vivo* experiment, the expression levels of GFP::SPD-5(Δ C1) and GFP::SPD-5(Δ C3) were several fold lower than the endogenous SPD-5 (Fig. S1A).

A dominant-negative effect of the CL+PA fragment (C1) also supports the importance of the intramolecular interactions between the PReM and the PA domains in the process of PCM expansion. The CL+PA fragment (C1) caused a dominant-negative effect on PCM expansion, whereas GFP::SPD-5(C-half), which contains a part of the PReM domain, in addition to the CL and the PA domains, did not. SPD-5(C1) interacted with both centriolar PCMD-1 and the PReM domain of SPD-5 and accumulated around the centrioles only in the presence of endogenous SPD-5, raising the possibility that over-accumulation of SPD-5(C1) with endogenous SPD-5 around the centrioles prevents the physical connection between the

centrioles and the PCM (Fig. 5C). Consistent with this hypothesis, the shape of the PCM in the GFP::SPD-5(C1)-expressing embryo resembled that in a *pcmd-1* mutant or the centriole-ablated condition that causes centriole–PCM connection defects in which the PCM is ripped apart by microtubule-mediated pulling forces (Erpf et al., 2019; Cabral et al., 2019). We speculate that a part of the PReM domain contained in GFP::SPD-5(C-half) is required for dissociation from centrioles, further implicating the requirement of intramolecular interactions between the PReM and the PA domains in the process of PCM expansion.

In this study, we demonstrated that SPD-5 is recruited to the centrioles through the interaction between its CL domain and centriolar PCMD-1. Previous studies proposed another model that SPD-5 binds throughout the pre-built PCM, then assembles into the PCM scaffold (Laos et al., 2015; Zwicker et al., 2014; Cabral et al., 2019). We speculate that these two routes of SPD-5 incorporation to the centrosome are not mutually exclusive and might reflect the two phases of mitotic PCM formation; at the beginning of mitotic PCM formation, SPD-5 is recruited to the centrioles in a PCMD-1-dependent manner, then once the PCM scaffold is assembled, SPD-5 can also be isotropically incorporated into the PCM.

Previous *in vitro* experiments suggested that SPD-5 plays a crucial role in PCM scaffold formation in *C. elegans*, which is dependent on phosphorylation-regulated interactions among coiled-coil proteins (Woodruff et al., 2017, 2015), but the involvement of specific domains has not been reported. Our results indicated that PLK-1 phosphorylation promotes specific interactions between the PReM and the PA domains of SPD-5 that are crucial for scaffold formation. Thus, PCM scaffold formation is not solely dependent on non-specific interactions between coiled-coil proteins, but rather, it requires well-organized, specific interactions.

Evolutionarily conserved mechanisms of PCM scaffold formation

SPD-5 has been thought to be a functional homolog of *Drosophila* Cnn and human CDK5RAP2, although sequence homology is undetectable (Fong et al., 2008; Hamill et al., 2002; Megraw et al., 1999).

Despite the lack of sequence similarity, Cnn and SPD-5 have some common features in their domain structures. Their N-termini have a binding domain for a γ -tubulin complex (Ohta et al., 2021; Zhang and Megraw, 2007). Both proteins have a domain for centrosomal targeting at their C terminus (CM2 for Cnn and CL for SPD-5) (Feng et al., 2017) and have a PReM domain in their central region that contains Polo/PLK-1 phosphorylation sites (Conduit et al., 2014a; Woodruff et al., 2015). Phosphorylation in the PReM domain by Polo/PLK-1 triggers the interaction between the PReM domain and a C-terminally located domain (CM2 for Cnn and PA for SPD-5), which leads to PCM scaffold assembly (Feng et al., 2017). Notably, the CM2 domain in Cnn carries out the combined roles of the CL and PA domains of SPD-5.

In conclusion, we have revealed the PCM scaffold assembly process mediated by SPD-5 through *in vivo* domain analyses. SPD-5 is recruited to the centrioles through direct interaction between its CL domain and PCMD-1. Phosphorylation by centriolar PLK-1 of the PReM domain of SPD-5 promotes its intramolecular and/or intermolecular interactions with the PA domain, which leads to mitotic PCM scaffold assembly. Our findings further suggest an evolutionarily conserved domain organization between Cnn and SPD-5, and their phosphorylation-dependent regulation. Further analysis of SPD-5 and other PCM proteins will lead to a better understanding of the universality and diversity of the PCM formation mechanisms.

MATERIALS AND METHODS

Worm strains and culture

All *C. elegans* strains were cultured as described (Brenner, 1974). The strains used in this article are listed in Table S1 and were maintained at 23°C.

Worm strain construction

Transgenes for GFP-tagged SPD-5 variants were inserted into the same genomic position with the MosSCI *ttTi5605* allele on chromosome II (Frøkjær-Jensen et al., 2008, 2012) by CRISPR/Cas9-mediated genome editing. We constructed a homologous repair template vector, pHK6, to insert SPD-5 variant transgenes into the *ttTi5605* site. pHK6 contains arms for homologous recombination at the *ttTi5605* site (Chr. II armL, 920 bp and armR, 967 bp), a GFP-encoding sequence under the control of the germline-specific *pie-1* promoter and 3' untranslated region (3'UTR), the self-excising cassette (SEC) (Dickinson et al., 2015) for hygromycin B selection and the *ccdB* sequence, which was substituted by each SPD-5 variant sequence (pHK6: Chr. II armL_ *pie-1*-p_coGFP_SEC_3×FLAG_ *ccdB*_ *pie-1* 3'UTR_Chr. II armR). The SEC_3×FLAG_ *ccdB* fragment was from pDD282 (Addgene #66823), except that the *let-858* 3'UTR was substituted by the *par-5* 3'UTR to prevent gene silencing in the germline. To construct homologous repair templates for SPD-5 variants, pHK6 was digested with *ApaI* restriction enzyme, which recognizes sites at both ends of the *ccdB* sequence, and the coding sequence for individual SPD-5 variants was assembled using the Gibson assembly method (Gibson et al., 2009).

For single guide RNA (sgRNA) expression, we constructed the pTK73 vector, which was modified from pRB1017 (Fire et al., 1998) to incorporate the sgRNA^(F+E) sequence (Chen et al., 2013). Then, the target sequence for the sgRNA (5'-GATATCAGTCTGTTTCGTAA-3') at the *ttTi5605* site was inserted into pTK73 (pTK73_ *ttTi5605*).

For the transgene insertion by CRISPR/Cas9, the following injection mixture was injected into N2 worms: the homologous repair templates (pHK6_ *spd-5* fragments, 10 ng/μl), the sgRNA plasmid (pTK73_ *ttTi5605*, 50 ng/μl), the Cas9 expression plasmid pDD162 (Peft-3::Cas9, 50 ng/μl, Addgene #47549) (Dickinson et al., 2013) and the three injection markers pCFJ90 (Pmyo-2::mCherry, Addgene #19327), pCFJ104 (Pmyo-3::mCherry, Addgene #19328) and pGH8 (Prab-3::mCherry, Addgene #19359) (Frøkjær-Jensen et al., 2008). Hygromycin B-resistant Roller worms that lacked mCherry fluorescence were selected as integrant candidates, and then were heat-shocked to remove the SEC. The integration and selection cassette excision were confirmed by sequencing.

Strain SA278 (mCherry::TBG-1; mCherry::Histone H2B) was constructed by microparticle bombardment (Toya et al., 2010). Dual-color strains [GFP::SPD-5(xx); mCherry::TBG-1; mCherry::Histone H2B] and [GFP::SPD-5(xx); mCherry::SAS-4] were constructed by crossing.

RNA interference

For the depletion of endogenous SPD-5 by RNA interference (RNAi), we used the sequence corresponding to the *spd-5* 3'UTR or an N-terminal open reading frame (ORF) region (1–1566 bp). For *pcmd-1* RNAi, we used the sequence corresponding to the ORF region (232–1079 bp). Template DNA fragments for synthesizing double-stranded RNAs (dsRNAs) were amplified by PCR. dsRNAs were synthesized *in vitro* with T7 RiboMAX Express Large Scale RNA Production System (Promega, Madison, USA) and then were purified by phenol–chloroform extraction. RNAi was carried out using the soaking method (Maeda et al., 2001). Briefly, 10 hermaphrodite early fourth larval stage (L4) worms were soaked in 2 mg/ml dsRNA solution and were incubated at 24.5°C for 24 h. Adult worms were then recovered from the dsRNA solution and incubated at 23°C on nematode growth medium (NGM) plates for 14–24 h before the worms were used for live imaging.

To permeabilize the eggshell for the *in vivo* PLK-1 inhibition assay, *perm-1* RNAi was performed by feeding method. An *E. coli* strain HT115 that expresses *perm-1* dsRNA was grown on NGM plates containing 1 mM isopropyl β -D-1-thiogalactopyranoside (IPTG) for 24 h at 23°C, and L4 worms were fed for 19–21 h at 20°C.

Microscopy

Fluorescence images were obtained as described (Honda et al., 2017) with an Orca-R2 digital CCD camera (Hamamatsu Photonics, Shizuoka, Japan) mounted on an IX71 microscope (Olympus, Tokyo, Japan) using a CSU-X1 spinning disc confocal system (Yokogawa Electric Corporation, Tokyo, Japan). MetaMorph software (Molecular Devices, CA, USA) was used to control the microscopes. Live images of one-cell embryos were obtained using a UPlanSApo 60×/1.30 silicone oil objective lens (Olympus) with camera gain 255 and binning 2, with 40 s intervals, 15 z-slices at intervals of 1 μm and a 300 ms exposure for GFP and 1000 ms exposure for mCherry. Immunofluorescence images were obtained using a UPlanSApo 100×/1.40 oil objective lens (Olympus) with camera gain 0 and without binning; with 20 z-slices at intervals of 0.5 μm and 250 ms exposure for Alexa Fluor 488, 100 ms exposure for Alexa Fluor 568 and 1000 ms exposure for DAPI. Images of the *pcmd-1(RNAi)* embryos and the *in vivo* PLK-1 inhibition assay were obtained using an ORCA-Flash4.0 V3 digital CMOS camera (Hamamatsu Photonics) on the same microscope system as above with a UPlanSApo 60×/1.30 silicone oil objective lens (Olympus), 40 z-slices at intervals of 0.5 μm and a 300 ms exposure for GFP and 1000 ms exposure for mCherry without binning.

Image analysis

ImageJ/Fiji software (NIH; <https://imagej.net/Fiji>) was used for processing and analyzing the obtained images. The distribution and diameter of centrosomal GFP signals (Fig. 1C; Fig. 3E; Fig. 4D; Fig. S1C,D) were measured using the Plot Profile tool along the short axis of embryos, and the average cytosolic signal was subtracted as the background. The diameter was defined as the length that exceeded the common threshold value. The area of centrosomal GFP signal (Fig. 1D) was calculated using the threshold set by the Yen algorithm.

Immunostaining

To generate antibodies against SPD-5 and PCMD-1, full-length recombinant SPD-5 or a PCMD-1 peptide (CDEGFDSSSLKNNPASLQRD; aa 6–24) was injected into rabbits as per standard protocols (MBL Life Science and Cosmo Bio, respectively).

For immunostaining, embryos were freeze cracked and fixed with –20°C methanol for 5 min and washed in 0.05% Tween 20 in phosphate-buffered saline (PBS-T). After being incubated for 30 min in PBS-T containing 0.1% bovine serum albumin (BSA) for blocking, the slides were incubated with rat anti-GFP (1:200, diluted with PBS-T containing 0.1% BSA; Nacalai Tesque, cat#04404-84, lot#M0P5692) and rabbit anti-SPD-5 (1:10,000; this study) or rabbit anti-PCMD-1 (1:10,000; this study) at 4°C overnight. Slides were washed with PBS-T and then were incubated with Alexa Fluor 488-conjugated donkey anti-rat IgG (1:500; Invitrogen, California, USA; RRID AB_2535794, lot# 2180272), Alexa Fluor 594-conjugated donkey anti-rabbit IgG (1:500; Invitrogen; RRID AB_141637, lot#52958A) and DAPI (1 mg/ml, 1:500; Dojinbo). After a 2 h incubation at room temperature, the slides were washed with PBS-T and mounted with ProLong Diamond (Thermo Fisher Scientific).

Scoring embryonic lethality

To score embryonic lethality, L4 worms were transferred to NGM plates with OP50 and incubated at 23°C for 24 h. Each 1-day-old adult was then transferred to a new plate and was allowed to lay eggs for 6 h before being removed. The plates with eggs were incubated at 23°C for 24 h, and the number of eggs and larvae was counted. The embryonic lethality was calculated as the number of eggs out of the total number of eggs and larvae.

Protein purification

PLK-1::6×His and 6×His::FLAG::SPD-5(C2) proteins used for the pull-down assay were obtained as follows: PLK-1::6×His was expressed in Sf9 insect cells and purified as described (Woodruff and Hyman, 2015). Briefly, PLK-1::6×His was expressed in Sf9 cells, and the cells were harvested 72 h after the infection of baculovirus generated by the Bac-to-Bac system (Invitrogen, cat#10359016). HisTALON Superflow Cartridge (Takara Bio, Shiga, Japan) was used for purification and the protein was eluted with

80 mM imidazole, and the buffer was then exchanged to imidazole-free buffer using PD-10 Columns (GE Healthcare). Proteins were concentrated using 30K Amicon Ultra Centrifugal Filters (Merck, Darmstadt, Germany).

6×His::FLAG::SPD-5(C2) was expressed in *E. coli* BL21-CodonPlus (DE3) (Agilent Technologies, CA, USA) using a cold-induced promoter (pCold, Takara Bio). Protein expression was induced by culturing for 18 h at 16°C with 0.5 mM IPTG. Flash-frozen bacterial pellets were dissolved in lysis buffer [20 mM HEPES, 1 mM DTT, 300 mM NaCl, 10% Glycerol, 1× cOmplete EDTA-free protease inhibitors (Roche, Basel, Switzerland) and PhosSTOP (Roche)] and sonicated (1 min, six times) before centrifugation (20,000 g, 30 min, 4°C). HisTrap HP (GE Healthcare) was used for purification and the protein was eluted with linear gradient from 25 to 500 mM imidazole, and the buffer was then exchanged to imidazole-free buffer and concentrated using 10K Amicon Ultra Centrifugal Filters (Merck).

Pull-down assay

GST, GST-tagged SPD-5(272–732_WT) or SPD-5(272–732_4A) bound to Glutathione Sepharose 4B beads were prepared as follows. The three proteins were expressed in *E. coli* in the same method as 6×His::FLAG::SPD-5(C2) described above. Bacterial pellets were dissolved in the binding buffer [PBS with 0.5 mM EDTA, 1 mM DTT, 1 mM PMSF, 26.3 μM MG-132 (Chemsene, New Jersey, USA), 2× cOmplete EDTA-free protease inhibitors (Roche), 1× PhosSTOP (Roche) and 1% TritonX-100], sonicated and centrifuged. The supernatant was filtered using a Millex-HV filter (0.45 μm; Merck) and incubated with Glutathione Sepharose 4B beads (GE Healthcare) for 2 h at 4°C. Beads were washed three times with the binding buffer.

Next, GST, GST-tagged SPD-5(272–732_WT) or SPD-5(272–732_4A) on Glutathione Sepharose 4B beads were treated by the purified PLK-1::6×His protein. The beads were incubated with or without 6.8 μM purified PLK-1::6×His in reaction buffer (25 mM HEPES, pH 7.4; 150 mM KCl; 0.5 mM DTT; 0.2 mM ATP; 10 mM MgCl₂; 0.025 mg/ml ovalbumin) (modified from Woodruff and Hyman, 2015). After a 60 min incubation at room temperature, the beads were washed three times with the C2-binding buffer (PBS with 150 mM NaCl, 0.5 mM EDTA, 1 mM DTT, 1 mM PMSF, 26.3 μM MG-132, 2× cOmplete EDTA-free protease inhibitors and 1% Triton X-100).

The beads with or without PLK-1 phosphorylation were incubated with 12.5 mM 6×His::FLAG::SPD-5(C2) at 4°C for 2 h. The beads were washed three times with the C2-binding buffer, then SDS-PAGE sample buffer (62.5 mM Tris-HCl, pH 6.8; 10% glycerol; 5% 2-mercaptoethanol; 2.5% SDS) was added. The samples were boiled at 98°C for 5 min and analyzed by western blotting.

In vivo PLK-1 inhibition assay

C. elegans eggs were permeabilized by *perm-1* RNAi, as described above. The worms were dissected in 43% egg buffer (25 mM HEPES pH 7.3, 118 mM NaCl, 48 mM KCl, 2 mM MgCl₂, 2 mM CaCl₂) (Toya et al., 2010) containing 1% DMSO or 10 μM PLK-1 inhibitor BI-2536 (diluted from 1 mM stock in DMSO; Selleckchem, TX, USA). Eggs at the stage of pronuclear appearance were observed 15 min after the mounting.

Western blotting

To check the expression level of transgenes, 15 one-day adult worms were collected in 10 μl of distilled water and flash-frozen in liquid nitrogen. The sample was then thawed and mixed with 3 μl of 4× SDS-PAGE sample buffer and 1.2 μl of 10% NP-40 and was boiled at 98°C for 5 min.

The samples were loaded onto a 5–20% gradient SDS-PAGE gel (Wako, Osaka, Japan) and transferred to an Immobilon-P Transfer Membrane (Merck). Antibodies were diluted with Signal Enhancer HIKARI for western blotting and enzyme-linked immunosorbent assays (ELISA; Nacalai Tesque). The primary antibodies rabbit anti-SPD-5 (1:2000) and rat anti-GFP (1:10,000) were generated against full-length recombinant proteins (MBL Life Science). Additional primary antibodies were rabbit anti-FLAG (1:2000; Sigma-Aldrich, MO, USA; cat#F7425, lot#078M4886V), mouse anti-GST B-14 (1:2000; Santa Cruz Biotechnology, TX, USA; cat#sc-138, lot#11009) and mouse anti- α -tubulin DM1A (1:2000; Sigma-Aldrich; cat#T9026, lot#029M4880V).

Secondary antibodies were horseradish peroxidase (HRP)-conjugated goat anti-mouse IgG (H+L) (1:50,000; Jackson ImmunoResearch Laboratories, Pennsylvania, USA; RRID AB_2338511, lot#93599), HRP-conjugated donkey anti-rabbit IgG (H+L) (1:50,000; Jackson ImmunoResearch Laboratories; RRID AB_10015282, lot#95427) and HRP-conjugated donkey anti-rat IgG (H+L) (1:50,000; Jackson ImmunoResearch Laboratories; RRID AB_2340638, lot#96323). Signals were detected using Chemi-Lumi One Ultra (Nacalai Tesque), and blot images were obtained with a ChemiDoc Touch MP (Bio-Rad, CA, USA). Images of full blots are shown in Fig. S4.

Yeast two-hybrid assay and screen

The ProQuest Two-Hybrid System (Invitrogen) was used for the yeast two-hybrid assays. Protein coding sequences were integrated into the plasmids pDEST22 and pDEST32 (Invitrogen, cat#PQ1000101), downstream of the GAL4 DNA-activation domain and DNA-binding domain, respectively. Yeast strain Mav203 (Invitrogen, cat#PQ1000101) was treated with Frozen-EZ Yeast Transformation II (Zymo Research, CA, USA) to generate competent cells and was then transformed with bait and prey plasmids. The transformants were selected by culturing on SC-Trp-Leu plates for 3 days at 30°C. Each yeast strain was cultured in 2 ml of liquid SC-Trp-Leu for 13 h at 30°C and was analyzed on selection plates containing 3-amino-1,2,4-triazole (3AT).

For the yeast two-hybrid screen, we first transformed yeast Mav203 with bait plasmids (the coding sequence of SPD-5 fragments or PCMD-1 subcloned into pDEST32) only and incubated the cells on SC-Trp plates. The competent yeast cells with a single bait vector were then used in a transformation with the prey vector (cDNA fragments cloned into a pPC86 plasmid, Invitrogen) for yeast two-hybrid screening. Transformation efficiency was measured based on the number of colonies on SC-Trp-Leu plates. For the screening, transformants were spread onto 20 SC-Trp-Leu+25 mM 3AT selection plates and incubated for 5–7 days at 30°C. Individual colonies were then picked and spread on new SC-Trp-Leu plates. As candidate interactors with SPD-5(C1), 21 colonies were obtained from 1.9×10^5 cells on selection plates. As candidate interactors with PCMD-1, 12 colonies were obtained from 6.6×10^4 cells on selection plates. The coding sequences of the candidate clones were PCR amplified and sequenced (Forward primer: 5'-TATAACGCGTTTGGAACTACT-3', Reverse primer: 5'-AGCCGACAACCTTGATTGGAGAC-3'), and their identities were determined by a WormBase BLAST/BLAT search (https://wormbase.org/tools/blast_blat). For all positive prey plasmids, interactions were confirmed by isolation from the positive colonies and re-transformation to Mav203 with the bait vector.

Statistical analysis

The details for quantification, sample numbers and statistical analyses are described in the main text, the figures and the figure legends. The values given for n represent the number of embryos imaged to determine phenotypes (Fig. 1A–D, Fig. 2A, Fig. 3D,E; Fig. S1C,D), the number of embryos counted to measure embryonic lethality (Fig. 2B) or the number of centrosomes imaged to determine phenotypes (Figs 3C, Fig. 4C,D).

GraphPad Prism 9 software was used to analyze and represent the data. Results are expressed as the mean value \pm s.d. (Fig. 1B–D, Fig. 3E, Fig. 4D) or the mean value \pm s.e.m. (Fig. 2B). One-way ANOVA and Tukey's multiple comparisons test were performed to determine significant differences (Fig. 1D, Fig. 2B). Significance levels: not significant, n.s., $P \geq 0.05$; * $P < 0.05$; ** $P < 0.01$; *** $P < 0.001$.

Acknowledgements

We thank Yuji Kohara (National Institute of Genetics, Mishima, Japan) for providing cDNA clones and the members of the Sugimoto laboratory for discussions.

Competing interests

The authors declare no competing or financial interests.

Author contributions

Conceptualization: A.S.; Methodology: M.N., H.K., K.T., N.H.; Formal analysis: M.N., H.K., N.H.; Investigation: M.N., H.K.; Writing - original draft: M.N.; Writing - review &

editing: N.H., A.S.; Supervision: N.H., A.S.; Project administration: A.S.; Funding acquisition: M.N., N.H., A.S.

Funding

This work was supported by Japan Society for the Promotion of Science (JSPS) KAKENHI Grant Numbers JP15H04369 and JP15K14503 and a Bilateral Joint Research Project to A.S.; JP16K07334 and JP20K06616 to N.H.; Ministry of Education, Culture, Sports, Science and Technology (MEXT)/JSPS World-leading Innovative & Smart Education (WISE) Program: Advanced Graduate Program for Future Medicine and Health Care, Tohoku University to M.N.

Peer review history

The peer review history is available online at <https://journals.biologists.com/jcs/article-lookup/doi/10.1242/jcs.259025>.

References

- Alvarez-Rodrigo, I., Steinacker, T. L., Saurya, S., Conduit, P. T., Baumbach, J., Novak, Z. A., Aydogan, M. G., Wainman, A. and Raff, J. W. (2019). Evidence that a positive feedback loop drives centrosome maturation in fly embryos. *eLife* **8**, e50130. doi:10.7554/eLife.50130
- Barr, A. R., Kilmartin, J. V. and Gergely, F. (2010). CDK5RAP2 functions in centrosome to spindle pole attachment and DNA damage response. *J. Cell Biol.* **189**, 23–39. doi:10.1083/jcb.200912163
- Brenner, S. (1974). The genetics of *Caenorhabditis elegans*. *Genetics* **77**, 71–94. doi:10.1093/genetics/77.1.71
- Cabral, G., Laos, T., Dumont, J. and Dammermann, A. (2019). Differential requirements for centrioles in mitotic centrosome growth and maintenance. *Dev. Cell* **50**, 355–366.e6. doi:10.1016/j.devcel.2019.06.004
- Chen, B., Gilbert, L. A., Cimini, B. A., Schnitzbauer, J., Zhang, W., Li, G.-W., Park, J., Blackburn, E. H., Weissman, J. S., Qi, L. S. et al. (2013). Dynamic imaging of genomic loci in living human cells by an optimized CRISPR/Cas system. *Cell* **155**, 1479–1491. doi:10.1016/j.cell.2013.12.001
- Conduit, P. T., Feng, Z., Richens, J. H., Baumbach, J., Wainman, A., Bakshi, S. D., Dobbelaere, J., Johnson, S., Lea, S. M. and Raff, J. W. (2014a). The centrosome-specific phosphorylation of Cnn by Polo/Plk1 drives Cnn scaffold assembly and centrosome maturation. *Dev. Cell* **28**, 659–669. doi:10.1016/j.devcel.2014.02.013
- Conduit, P. T., Richens, J. H., Wainman, A., Holder, J., Vicente, C. C., Pratt, M. B., Dix, C. I., Novak, Z. A., Dobbie, I. M., Schermelleh, L. et al. (2014b). A molecular mechanism of mitotic centrosome assembly in *Drosophila*. *eLife* **3**, e03399. doi:10.7554/eLife.03399
- Decker, M., Jaensch, S., Pozniakovskiy, A., Zinke, A., O'Connell, K. F., Zachariae, W., Myers, E. and Hyman, A. A. (2011). Limiting amounts of centrosome material set centrosome size in *C. elegans* embryos. *Curr. Biol.* **21**, 1259–1267. doi:10.1016/j.cub.2011.06.002
- Dickinson, D. J., Ward, J. D., Reiner, D. J. and Goldstein, B. (2013). Engineering the *Caenorhabditis elegans* genome using Cas9-triggered homologous recombination. *Nat. Methods* **10**, 1028–1034. doi:10.1038/nmeth.2641
- Dickinson, D. J., Pani, A. M., Heppert, J. K., Higgins, C. D. and Goldstein, B. (2015). Streamlined genome engineering with a self-excising drug selection cassette. *Genetics* **200**, 1035–1049. doi:10.1534/genetics.115.178335
- Erpf, A. C., Stenzel, L., Memar, N., Antonioli, M., Osepashvili, M., Schnabel, R., Conradt, B. and Mikeladze-Dvali, T. (2019). PCMD-1 organizes centrosome matrix assembly in *C. elegans*. *Curr. Biol.* **29**, 1324–1336.e6. doi:10.1016/j.cub.2019.03.029
- Feng, Z., Caballe, A., Wainman, A., Johnson, S., Haensele, A. F. M., Cottee, M. A., Conduit, P. T., Lea, S. M. and Raff, J. W. (2017). Structural basis for mitotic centrosome assembly in flies. *Cell* **169**, 1078–1089.e13. doi:10.1016/j.cell.2017.05.030
- Fire, A., Xu, S., Montgomery, M. K., Kostas, S. A., Driver, S. E. and Mello, C. C. (1998). Potent and specific genetic interference by double-stranded RNA in *Caenorhabditis elegans*. *Nature* **391**, 806–811. doi:10.1038/35888
- Fong, K.-W., Choi, Y.-K., Rattner, J. B. and Qi, R. Z. (2008). CDK5RAP2 is a pericentriolar protein that functions in centrosomal attachment of the γ -tubulin ring complex. *Mol. Biol. Cell* **19**, 115–125. doi:10.1091/mbc.e07-04-0371
- Frøkjær-Jensen, C., Davis, M. W., Hopkins, C. E., Newman, B. J., Thummel, J. M., Olesen, S.-P., Grunnet, M. and Jorgensen, E. M. (2008). Single-copy insertion of transgenes in *Caenorhabditis elegans*. *Nat. Genet.* **40**, 1375–1383. doi:10.1038/ng.248
- Frøkjær-Jensen, C., Davis, M. W., Ailion, M. and Jorgensen, E. M. (2012). Improved Mos1-mediated transgenesis in *C. elegans*. *Nat. Methods* **9**, 117–118. doi:10.1038/nmeth.1865
- Giansanti, M. G., Bucciarelli, E., Bonaccorsi, S. and Gatti, M. (2008). *Drosophila* SPD-2 is an essential centriole component required for PCM recruitment and astral-microtubule nucleation. *Curr. Biol.* **18**, 303–309. doi:10.1016/j.cub.2008.01.058

- Gibson, D. G., Young, L., Chuang, R.-Y., Venter, J. C., Hutchison, C. A. and Smith, H. O.** (2009). Enzymatic assembly of DNA molecules up to several hundred kilobases. *Nat. Methods* **6**, 343-345. doi:10.1038/nmeth.1318
- Gomez-Ferreira, M. A., Rath, U., Buster, D. W., Chanda, S. K., Caldwell, J. S., Rines, D. R. and Sharp, D. J.** (2007). Human Cep192 is required for mitotic centrosome and spindle assembly. *Curr. Biol.* **17**, 1960-1966. doi:10.1016/j.cub.2007.10.019
- Hamill, D. R., Severson, A. F., Carter, J. C. and Bowerman, B.** (2002). Centrosome maturation and mitotic spindle assembly in *C. elegans* require SPD-5, a protein with multiple coiled-coil domains. *Dev. Cell* **3**, 673-684. doi:10.1016/S1534-5807(02)00327-1
- Haren, L., Stearns, T. and Lüders, J.** (2009). Plk1-dependent recruitment of γ -tubulin complexes to mitotic centrosomes involves multiple PCM components. *PLoS One* **4**, e5976. doi:10.1371/journal.pone.0005976
- Honda, Y., Tsuchiya, K., Sumiyoshi, E., Haruta, N. and Sugimoto, A.** (2017). Tubulin isotype substitution revealed that isotype combination modulates microtubule dynamics in *C. elegans* embryos. *J. Cell Sci.* **130**, 1652-1661. doi:10.1242/jcs.200923
- Kemp, C. A., Kopish, K. R., Zipperlen, P., Ahringer, J. and O'Connell, K. F.** (2004). Centrosome maturation and duplication in *C. elegans* require the coiled-coil protein SPD-2. *Dev. Cell* **6**, 511-523. doi:10.1016/S1534-5807(04)00066-8
- Laos, T., Cabral, G. and Dammermann, A.** (2015). Isotropic incorporation of SPD-5 underlies centrosome assembly in *C. elegans*. *Curr. Biol.* **25**, R648-R649. doi:10.1016/j.cub.2015.05.060
- Maeda, I., Kohara, Y., Yamamoto, M. and Sugimoto, A.** (2001). Large-scale analysis of gene function in *Caenorhabditis elegans* by high-throughput RNAi. *Curr. Biol.* **11**, 171-176. doi:10.1016/S0960-9822(01)00052-5
- Megraw, T. L., Li, K., Kao, L. R. and Kaufman, T. C.** (1999). The centrosomin protein is required for centrosome assembly and function during cleavage in *Drosophila*. *Development* **126**, 2829-2839. doi:10.1242/dev.126.13.2829
- Ohta, M., Zhao, Z., Wu, D., Wang, S., Harrison, J. L., Gómez-Cavazos, J. S., Desai, A. and Oegema, K. F.** (2021). Polo-like kinase 1 independently controls microtubule-nucleating capacity and size of the centrosome. *J. Cell Biol.* **220**, e202009083. doi:10.1083/jcb.202009083
- Palazzo, R. E., Vogel, J. M., Schnackenberg, B. J., Hull, D. R. and Wu, X.** (2000). Centrosome maturation. *Curr. Top. Dev. Biol.* **49**, 449-470. doi:10.1016/S0070-2153(99)49021-0
- Pelletier, L., Özlü, N., Hannak, E., Cowan, C., Habermann, B., Ruer, M., Müller-Reichert, T. and Hyman, A. A.** (2004). The *Caenorhabditis elegans* centrosomal protein SPD-2 is required for both pericentriolar material recruitment and centriole duplication. *Curr. Biol.* **14**, 863-873. doi:10.1016/j.cub.2004.04.012
- Stenzel, L., Schreiner, A., Zucconi, E., Üstüner, S., Mehler, J., Zanin, E. and Mikeladze-Dvali, T.** (2021). PCMD-1 bridges the centrioles and the pericentriolar material scaffold in *C. elegans*. *Development* **148**, dev198416. doi:10.1242/dev.198416
- Toya, M., Iida, Y. and Sugimoto, A.** (2010). Imaging of mitotic spindle dynamics in *Caenorhabditis elegans* embryos. *Methods Cell Biol.* **97**, 359-372. doi:10.1016/S0091-679X(10)97019-2
- Woodruff, J. B. and Hyman, A. A.** (2015). Chapter 19 - Method: in vitro analysis of pericentriolar material assembly. *Methods Cell Biol.* **129**, 369-382. doi:10.1016/bs.mcb.2015.04.006
- Woodruff, J. B., Wueseke, O., Viscardi, V., Mahamid, J., Ochoa, S. D., Bunkenborg, J., Widlund, P. O., Pozniakovsky, A., Zanin, E., Bahmanyar, S. et al.** (2015). Centrosomes. Regulated assembly of a supramolecular centrosome scaffold in vitro. *Science* **348**, 808-812. doi:10.1126/science.aaa3923
- Woodruff, J. B., Ferreira Gomes, B., Widlund, P. O., Mahamid, J., Honigsmann, A. and Hyman, A. A.** (2017). The centrosome is a selective condensate that nucleates microtubules by concentrating tubulin. *Cell* **169**, 1066-1077.e10. doi:10.1016/j.cell.2017.05.028
- Wueseke, O., Zwicker, D., Schwager, A., Wong, Y. L., Oegema, K., Jülicher, F., Hyman, A. A. and Woodruff, J. B.** (2016). Polo-like kinase phosphorylation determines *Caenorhabditis elegans* centrosome size and density by biasing SPD-5 toward an assembly-competent conformation. *Biol. Open* **5**, 1431-1440. doi:10.1242/bio.020990
- Zhang, J. and Megraw, T. L.** (2007). Proper recruitment of γ -tubulin and D-TACC/ Msps to embryonic *Drosophila* centrosomes requires Centrosomin Motif 1. *Mol. Biol. Cell* **18**, 4037-4049. doi:10.1091/mbc.e07-05-0474
- Zwicker, D., Decker, M., Jaensch, S., Hyman, A. A. and Jülicher, F.** (2014). Centrosomes are autocatalytic droplets of pericentriolar material organized by centrioles. *Proc. Natl. Acad. Sci. USA* **111**, E2636-E2645. doi:10.1073/pnas.1404855111